1

Opportunity Research Scholars' Program

School of Electrical and Computer Engineering
Georgia Institute of Technology

Audio Spoof Detection with Mel Frequency Cepstral Coefficients and Gaussian Mixture Models

Acoustics Lab
David Anderson

Semiconductor Research Corporation

Akhil Gazula, Vincent Wang, David Yu, PhD Mentor: Chuyao Feng, Faculty: David Anderson

School of Electrical and Computer Engineering • Georgia Institute of Technology • Atlanta GA, 30332 USA

Introduction

- Increasing number of robocalls
- Current call blocking techniques are inadequate as they rely on caller IDs
- We focus on the audio of the call and built a speaker verification tool that can differentiate robocalls and real voices
- Mel Frequency Cepstral Coefficients (MFCCs) capture features of speaker's voice
- Train a Gaussian Mixture Model (GMM) with the features

Experiment

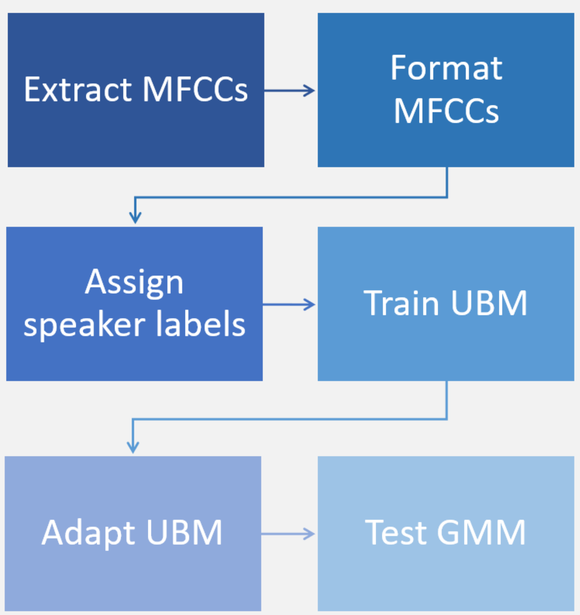

Results

Initial Testing

Speaker Verification Likelihood

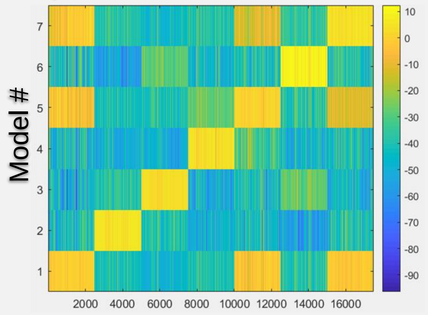

Equal Error Rate (EER)

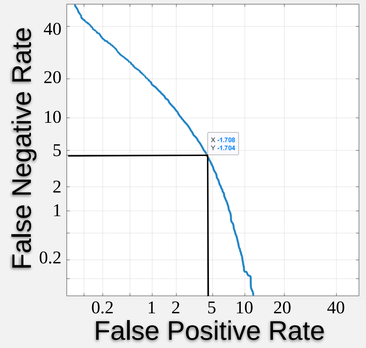

Cross Evaluation Results

Speaker Verification Likelihood

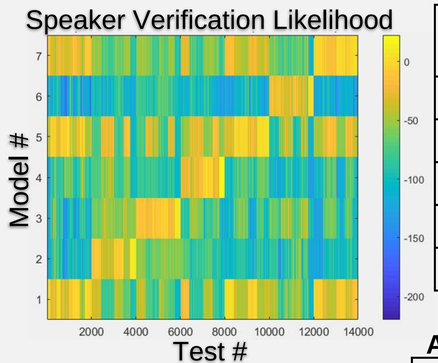

Above is the Trial 5 speaker verification likelihood.

Trial Number	Training Group	Equal Error Rate (EER)
1	Group 1	39.67%
2	Group 2	43.97%
3	Group 3	43.31%
4	Group 4	38.92%
5	Group 5	46.12%

All Trials

Mean Equal Error Rate	42.40%
Standard Deviation	3.03%

Discussion

- Models 5 and 7 (spoof types) were classified as similar to Model 1 (real speaker) for both tests
- Initial testing using identical training and test data results in EER of 5%
- Cross evaluation results are significantly worse, EER 37.4% higher than initial test result

Conclusions

- Most spoof types can be detected
- Model can effectively differentiate speakers, but high EER implies it cannot reliably determine the correct speaker
- Model needs improvement

Future Work

- Improve model accuracy and decrease EER
- Apply model to other audio sources like bird sounds
- Explore other audio features like IMFCC and LFCC that may improve model performance

References

AARP. "How to Stop Illegal Robocalls: Tips and Resources." *AARP*, 14 May 2019.

Jones, Rupert. "Voice Recognition: Is It Really as Secure as It Sounds?" *The Guardian*, Guardian News and Media, 22 Sept. 2018.

Kofman, Ava. "Interpol Rolls Out International Voice Identification Database Using Samples From 192 Law Enforcement Agencies." *The Intercept*, 25 June 2018.

Mak, M. and Chien, J. INTERSPEECH 2016 Tutorial: Machine Learning for Speaker Recognition.

Georgia Tech School of Electrical and Computer Engineering
College of Engineering

2

Opportunity Research Scholars' Program

School of Electrical and Computer Engineering
Georgia Institute of Technology

Hiding Data in Sound

Communication Theory Research Group

John R. Barry

Rahil Ajani, Kombundit Chitranuwatkul, Harley Ovell
Mentor: Derrick Chu
School of Electrical and Computer Engineering • Georgia Institute of Technology • Atlanta GA, 30332 USA

Introduction

- High data rate in acoustic communication system
- Data embedded within an existing cover audio signal
- Imperceptible to human listener
- Commercial-off-the-shelf speakers and microphone

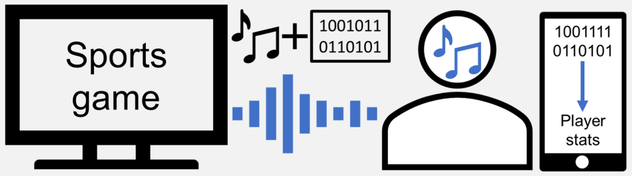

Figure 1. An application of hiding data in a live stream sport game.

- Secondary data stream within cover audio signal
- Applications: Sports statistics, advertisement information, exclusive coupons

Background

- Existing approaches:
  - Spread spectrum communications - imperceptible but low data rate
  - Ultrasonic communications - imperceptible, large bandwidths, but requires special equipment

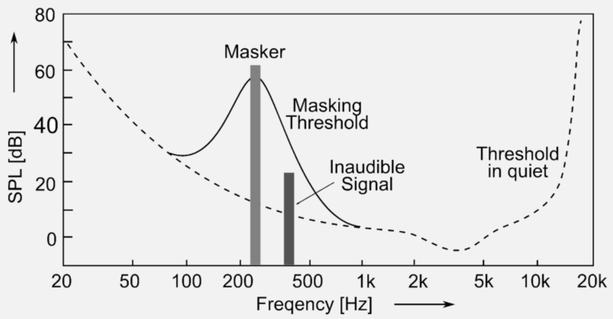

Figure 2. An example of psychoacoustic masking curve from a tonal excitation [6].

Approach

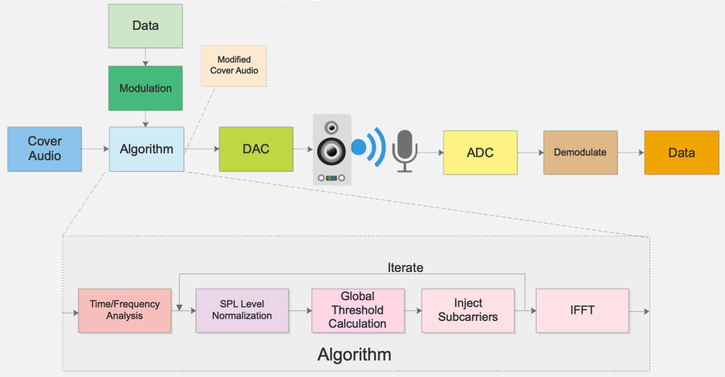

Figure 3. System level and algorithm block diagram.

- Algorithm analyzes cover audio, identifies components to be removed, then injects OFDM subcarriers.
- Receiver demodulates data signal embedded in cover audio. Receiver assumed to have knowledge of subcarrier positions.

Experiments

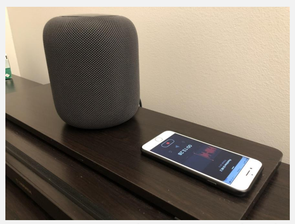

Figure 4. Acoustic communication experimental setup.

- Speaker transmits data embedded in cover audio
- Smartphone records audio, then off loads to computer for decoding

- Hidden data criteria is tested with human participants.
- Given a random combination of original and modified audio.
  -Participants asked if there is a difference
  -Rates difference on 1-10 scale

n = 10	Difference (%)	No Difference (%)	Avg Difference Score
Same sample pair (O,O) and (M,M)	40%	60%	1.3
Different sample pair (O,M) and (M,O)	65%	35%	2.2

Conclusions

- Developed an algorithm that identifies cover audio frequencies to be replaced with data subcarriers. Presently does not satisfy hidden data constraint, but perceived difference is small on 1-10 scale.
- Efficient implementation of OFDM transmitter which directly replaces cover audio FFT coefficients with data subcarriers.

Future Work

- Experiment with more participants
- Improve carrier injection algorithm
- Improve receiver design
- Bit-loading for OFDM subcarriers to improve data rate
- Adjust model to accomodate for Multiple-Input Multiple-Output (MIMO)
- Develop mobile phone application

Figure 5. Multiple microphones on a smartphone for MIMO.

References

[1] M. Zhou, Q. Wang, K. Ren, D. Koutsonikolas, L. Su and Y. Chen, "Dolphin: Real-Time Hidden Acoustic Signal Capture with Smartphones," in *IEEE Transactions on Mobile Computing*, vol. 18, no. 3, pp. 560-573, 1 March 2019. doi: 10.1109/TMC.2018.2842771

[2] Olson, Harry F. (1967). *Music, Physics and Engineering*. Dover Publications. pp. 248–251. ISBN 978-0-486-21769-7.

[3] Pan, D. "A Tutorial on MPEG/Audio Compression." *IEEE Multimedia*, vol. 2, no. 2, 1995, pp. 60–74., doi:10.1109/93.388209.

[4] Perceptual model-based information hiding in audio signals - Scientific Figure on ResearchGate. Available from: https://www.researchgate.net/figure/Frequency-masking-in-the-human-auditory-system-HAS_fig1_233893607

[5] Matsuoka, Hosei & Nakashima, Yusuke & Yoshimura, Takeshi & Kawahara, Toshiro. (2008). Acoustic OFDM: Embedding high bit-rate data in audio. 4903. 498-507. 10.1007/978-3-540-77409-9_47.

[6] Herre, Jürgen & Dick, Sascha. (2019). Psychoacoustic Models for Perceptual Audio Coding—A Tutorial Review. Applied Sciences. 9. 2854. 10.3390/app9142854.

Georgia Tech School of Electrical and Computer Engineering
College of Engineering

3

School of Electrical and Computer Engineering
College of Engineering

ORS
Opportunity Research Scholars' Program
School of Electrical and Computer Engineering
Georgia Institute of Technology

Parallel Path Signal Transmission for Capacity and Reliability Enhancement

Shelby Crisp, Abigail Drun, Yue Teng, Rob Walker
PhD Mentor: Shang-Jen Su, Faculty Advisor: Gee-Kung Chang

Introduction

The purpose of this project is to enhance the capacity and reliability of communication systems to fulfill the growing demand for a faster, more reliable network with greater bandwidth.

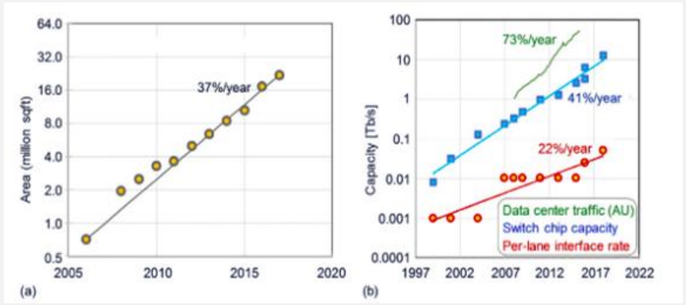

Figure 1. (a) Aggregate data center footprint in millions of square feet for four major cloud providers as a function of time; (b) Growth rate of Broadcom Ethernet switch capacities and line rates as a function of time, reported by google [1]

A parallel path signal transmission architecture is being implemented, combining:

- A fiber-optic transmission path
  - Good bandwidth and transmission distance
  - Longer to set up
- A free-space optical (FSO) transmission path
  - More prone to noise and distance limited
  - Easy to set up

Experiment

VPIphotonics (VPI) was chosen for the fiber-optic communication system simulation because of the fiber-based components it includes.
MATLAB was used for PAM4 modulation, adaptive filtering, and demodulation.
The signal after modulation was imported to VPI as the input for the VPI simulation. The simulation output was exported from VPI and imported to MATLAB for adaptive filtering and demodulation.

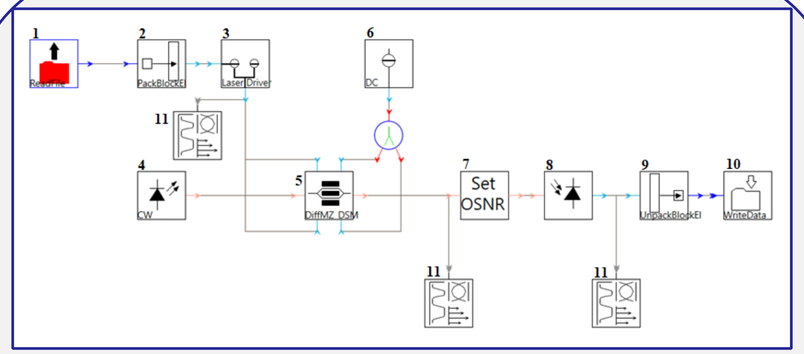

Figure 2. Schematic of VPI simulation with blocks: 1. file reader (reads external input file); 2. digital signal to electrical signal converter; 3. laser driver; 4. laser; 5. Mach-Zehnder modulator; 6. DC power supply; 7. user-defined OSNR; 8. photodetector; 9. Electrical signal to digital signal converter; 10. Data writer (exports output to external file); 11. Signal Analyzer.

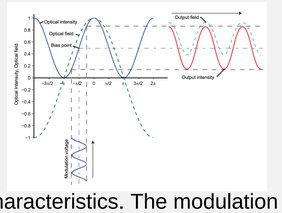

Figure 3. MZM transfer characteristics. The modulation is sinusoidal with ε = −0.5 (quadrature biasing) and α = 0.5 (normalized amplitude of driving voltage).[2]

Results

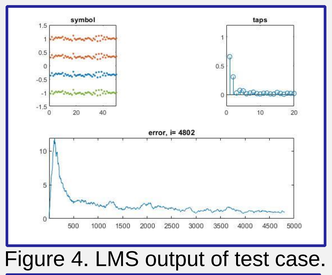

Figure 4. LMS output of test case.

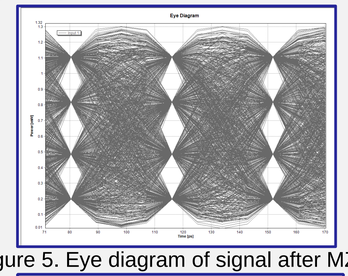

Figure 5. Eye diagram of signal after MZM.

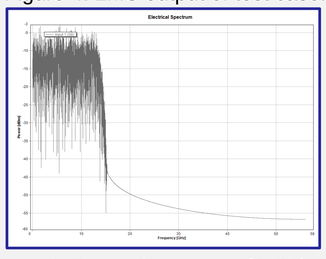

Figure 6. Power Spectrum of VPI input.

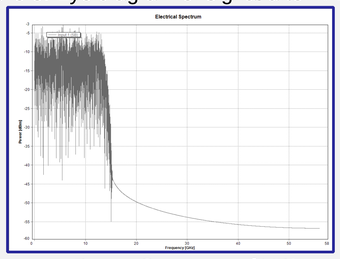

Figure 7. Power Spectrum of VPI output with OSNR set to 999 and transmission distance set to zero..

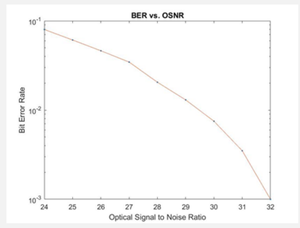

Figure 8. Plot of BER vs. OSNR for VPI simulation over zero transmission distance.

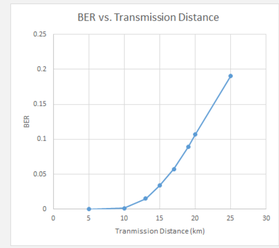

Figure 9. Plot of BER vs. transmission distance for VPI simulation with OSNR set to 32 dB.

Conclusions

LMS filter error decreases as it adapts, indicating that the filter works as it should.
Eye diagram indicates signal after MZM is clear.
Comparison of power spectrums shows that the signal doesn't change much during transmission, so the signal was successfully transmitted with little error when the OSNR is set to 999.

- Future work:
  - LMS optimization
  - Test FSO transmission path on hardware
  - Integrate fiber-optic communication system and FSO communication system

References

[1] P. J. Winzer, D. T. Neilson, and A. R. Chraplyvy, "Fiber-optic transmission and networking: the previous 20 and the next 20 years [Invited]," Optics Express, vol. 26, no. 18, p. 24190, 2018.
[2] Generation, Modulation, and Detection of Signals in Microwave Photonic Systems - Scientific Figure on ResearchGate. Available from: https://www.researchgate.net/figure/MZM-transfer-characteristics-The-modulation-is-sinusoidal-according-to-Eq-22-with-e_fig5_230559643 [accessed 30 Mar, 2020]

4

Traversing the Latent Space of Generative Models using Paired Comparisons

Mark Faingold, Miguel Garcia, Jason Palmer, Matthew O'Shaughnessy, Mark Davenport, and Christopher Rozell

ORS Opportunity Research Scholars' Program
School of Electrical and Computer Engineering
Georgia Institute of Technology

Georgia Tech School of Electrical and Computer Engineering
College of Engineering

Raytheon

Georgia Tech

Motivation

Variational autoencoders are a ***deep generative model*** capable of producing photorealistic images from a given dataset. We wish to create an application allowing users to produce a desired image from this model without needing an in-depth understanding of the model.

The problem being solved takes the form of:

$$\text{user } \boldsymbol{x} \text{ prefers point } \boldsymbol{q}_i \text{ over point } \boldsymbol{q}_j$$

where points q_i and q_j have a corresponding output image.

The model consists of an ***encoder*** **and** ***decoder.*** The encoder converts data from a high-dimensional space, such as the image space, to a low-dimensional feature representation known as the ***latent space.*** The low-dimensional representation is then transformed back to the real space via the ***decoder***. Figure 1 shows this process with the MNIST digits dataset [1]. Despite being relatively low-dimensional compared to the image space, the latent space still consists of many dimensions, making it difficult for humans to analyze.

Input Dataset **Sampling from the Latent Space after 250 Epochs of Training**

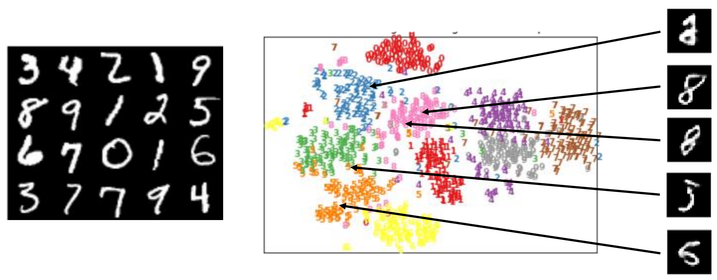

Figure 1. Visualization of a Variational Autoencoder. An input image is encoded into a low-dimensional probabilistic feature space known as the latent space. Afterwards, an embedding is sampled and decoded back into the image space, creating an entirely new image [3].

Additionally, it is a non-trivial problem to provide humans with the necessary intuition to describe desired features in mathematical terms, as described below in Figure 2. This problem is only amplified when trying to describe desired features in the latent space of a high dimensional generative model [2].

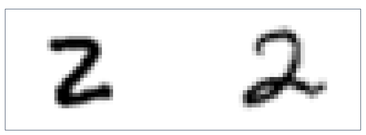

Figure 2. Two variants of the MNIST digit '2' produced from a Variational Autoencoder. How does the user describe in numerical terms if the "flat two" is preferred over the "curly two"?

Contribution: Localizing Desired Features Within the Latent Space of a VAE using Paired Comparisons

Optimization Problem

$$\min_{x^*,\xi} \frac{1}{2}\|x^* - x_0\| + \sum_k C_k \xi_k$$
$$\text{s.t. } \left\|x^* - q_i^k\right\|_2^2 \le \left\|x^* - q_j^k\right\|_2^2 + \xi k$$
$$\xi k \ge 0$$

In this convex optimization problem, x^* represents an *ideal point*, q_i represents the "closer" comparison, and q_j represents the "further" comparison.

2D Visualization with MNIST digits

Example of a Paired Comparison

q_j, further **q_i, closer**

Figure 3. Example of a paired comparison from the StyleGAN faces dataset. The user wishes to localize the point corresponding to an "old man with gray hair."

Effect of Comparisons on Localizing a Digit **"Best" Found Point**

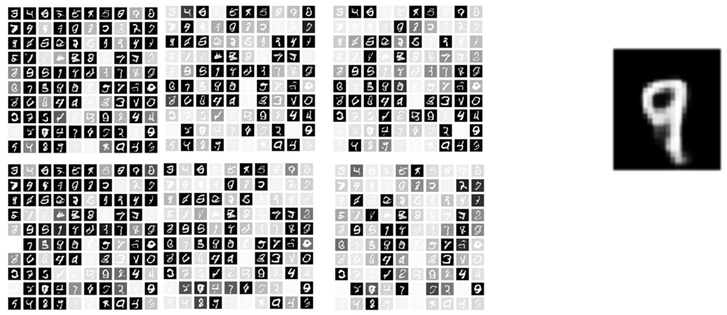

Figure 4. Gallery of 100 generated images, showing that once a user makes a comparison, the gallery fades proportionally to the Euclidean distance from the updated ideal point x^*.

Localizing a "6" from the MNIST Digit Set after 25 Comparisons

T-SNE Embedding of Latent Space **Localized Point**

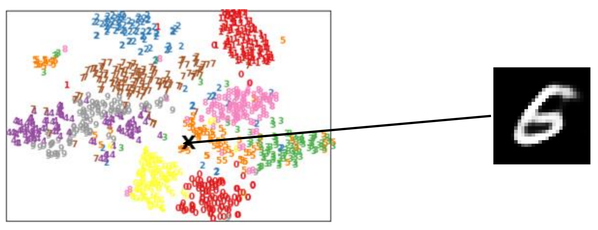

Figure 5. T-SNE embedding plot with 'X' showing the localized point in both latent and image space; yellow cluster represents a region composed of "sixes" [3].

Applications

Human Preference Quantization:

Humans are notoriously bad at consistently quantifying their natural responses; in contrast, they have accurate intuition about non-metric data [4].

- Choosing foods, fonts, etc.
- Shoe model
- Remembering songs
- Application: Daily Life

Figure 6. Zappos sandals dataset used to generate photorealistic images of sandals

Vocabulary for Understanding Systems with High Dimensions

There are many cases in which humans understand a desired feature of a system, but lack the vocabulary to provide accurate descriptions.

- User-interface code synthesis
- Voice generation
- Generation of desired products
- Analyze cybersecurity trends

An Interface for Future Learning

The ability of paired comparisons to accurately localize desired characteristics allows for itself to be a useful interface for future work on the topic of generative models. For instance, this method of traversing the latent space can be used in order to learn more about the structure of the latent space of GANs. Additionally, paired comparisons are a viable means of data augmentation for topics where training data is rare or expensive.

Future Work

Graphical User Interface

- Integrated GUI program for users to interface with paired comparison model and algorithm

User Survey

- Implement application to conduct an Amazon Mechanical Turk study on StyleGAN pretrained models

References

[1] Canal, Massimino, Davenport, and Rozell, "Active embedding search via noisy paired comparisons," in Proc. ICML, 2019"

[2] "Davenport, "Lost without a compas: Nonmetric traingulation and landmark multidimensional scaling," in Proc. IEEE CAMSAP 2013"

[3] Gleicher, Leitte, and Viola. Latent space cartography: Visual analysis of vector space embeddings. The Eurographics Association, 2019.

[4] M R O'Shaughnessy and M A Davenport. Localizing users and items from paired comparisons. In *2016 IEEE 26th International Workshop on Machine Learning for Signal Processing* (MLSP), pages 1–6. IEEE, 2016.

5

t Generation Transparent Rectifying Antenna Design for Space Solar Power

Erik Centeno, Alaina Do, Rafael Figueroa, Evan Shi, Lycia Tran | PhD Mentor: Cheng Qi | Faculty Advisor: Dr. Gregory Durgin

The Propagation Group

Georgia Tech School of Electrical and Computer Engineering
College of Engineering

ORS Opportunity Research Scholars' Program
School of Electrical and Computer Engineering
Georgia Institute of Technology

SSP as a Renewable

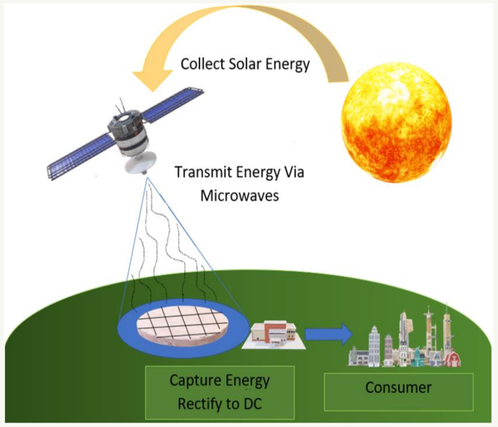

Figure 1. Space Solar Power (SSP) transmits power wirelessly at microwave frequencies to Earth from a solar collection satellite [1].

Pros:

- Uninterrupted, renewable energy
- Can provide large amount of power

Cons:

- Complex, expensive implementation

SSP is a promising alternative energy source that needs to display economic feasibility to the general public and policy makers.

Objective

Reduce Space Solar Power ground station cost to increase commercial feasibility by:

- Replacing the ground plane of working prototype with wire mesh to increase transparency
- Redesigning antenna to improve gain and decrease loss
- Moving from glass to less fragile acrylic substrate

Simulation

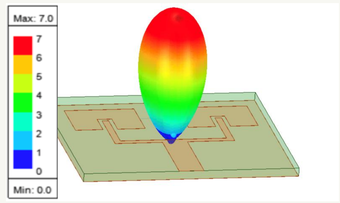

Figure 2 (left): 2x1 patch antenna array and gain pattern plotted in HFSS. Max gain is **7 dBi**.

Figure 3 (right): Charge pump layout from EAGLE, showing matching stubs and attachment points for discrete components.

Cost Analysis

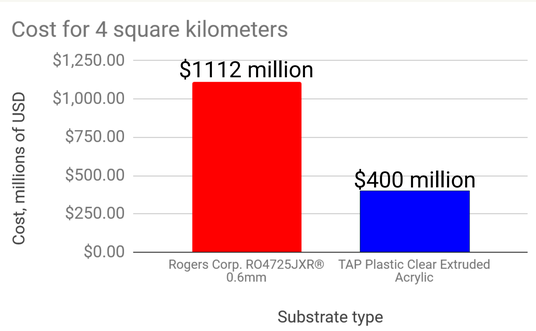

Figure 4: Acrylic substrate is nearly 2.8 times less expensive than the typically used, optimized RO4725JXR substrate.

Fabrication

Step 1: Place copper tape over glass. Trace rectenna design stencil with sharp blade.

Step 2: Remove excess copper foil from outline.

Step 3: Attach wire mesh with tape and form electrical connections.

Step 4: Join discrete components onto copper tape using non conductive adhesive strips.

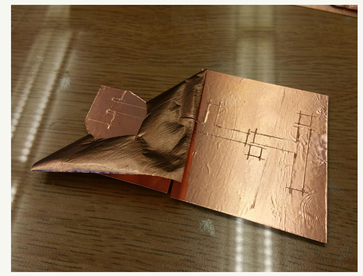

Results

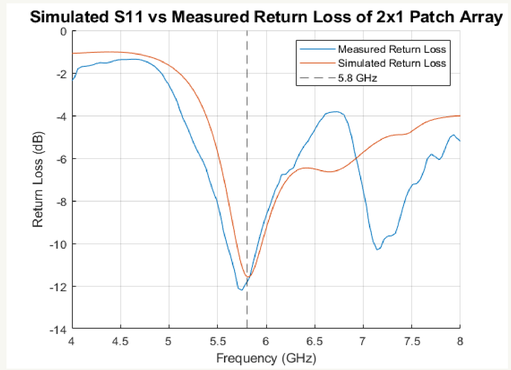

Figure 5 (above): Simulated and measured return loss for new antenna design. **Figure 6 (below)**: Transparency comparison between solid and meshed ground planes.

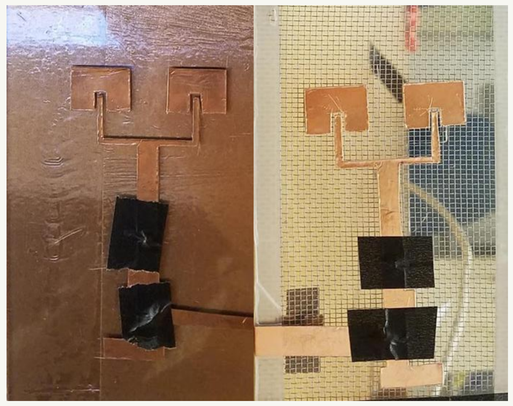

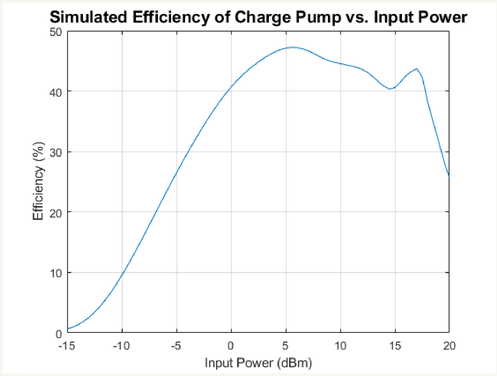

Figure 7 (above): Simulated charge pump conversion efficiency versus input power level.

Given 700W (~58.5 dBm) transmit power at 5.8GHz, 10 meter separation (-67.7 dB loss), ~20 dBi transmit gain, ~7 dBi receive gain:

Power input for a single charge pump:

P_{input} = 58.5 + 20 + 7 - 67.7= 17.8 dBm

= **0.66W per charge pump**

~43% efficiency: 0.28W DC available per rectenna

Observations

- Efficiency and output power improved due to increased antenna aperture in new 2x1 patch array antenna.
- Measured return loss at 5.8 GHz is -12 dB for antenna with solid ground plane.
- Materials used yield an inexpensive and rapid manufacturing technique.
- Rectenna still functional with mesh ground plane

Future Work

1) Collect additional data for meshed rectenna.
2) Optimize array size to deliver maximum power acceptable for diode.
3) Conduct high power magnetron test.
4) Determine geometric deviation between antenna fabrications.

References

[1] J. McSpadden and J. Mankins, "Space solar power programs and microwave wireless power transmission technology", IEEE Microwave Magazine, vol. 3, no. 4, pp. 46-57, 2002.

6

Opportunity Research Scholars' Program

School of Electrical and Computer Engineering
Georgia Institute of Technology

Audio Classification into Musical Tones Using Mixed Signal Processing

Computational Electronics Laboratory (ICE)
Dr. Jennifer Hasler

Adrija Bhattacharya | Justin Kelley | Albert Zhi

PhD Mentor: Aishwarya Natarajan | Faculty Advisor: Dr. Jennifer Hasler

School of Electrical and Computer Engineering • Georgia Institute of Technology • Atlanta GA, 30332 USA

Project Goal:

This project's goal is to build a circuit for the System-on-Chip (SoC) FPAA that converts raw audio input into distinct musical tones. This is achieved through an analog bank of bandpass filters feeding data into a classifier, whose output will determine the note.

About the FPAA:

The Field Programmable Analog Array (FPAA) is a mixed signal device that can operate at 1000x the power efficiency as a traditional FPGA. This is achieved via combining analog and digital elements into a single fabric, which is programmed by floating-gate technology[1].

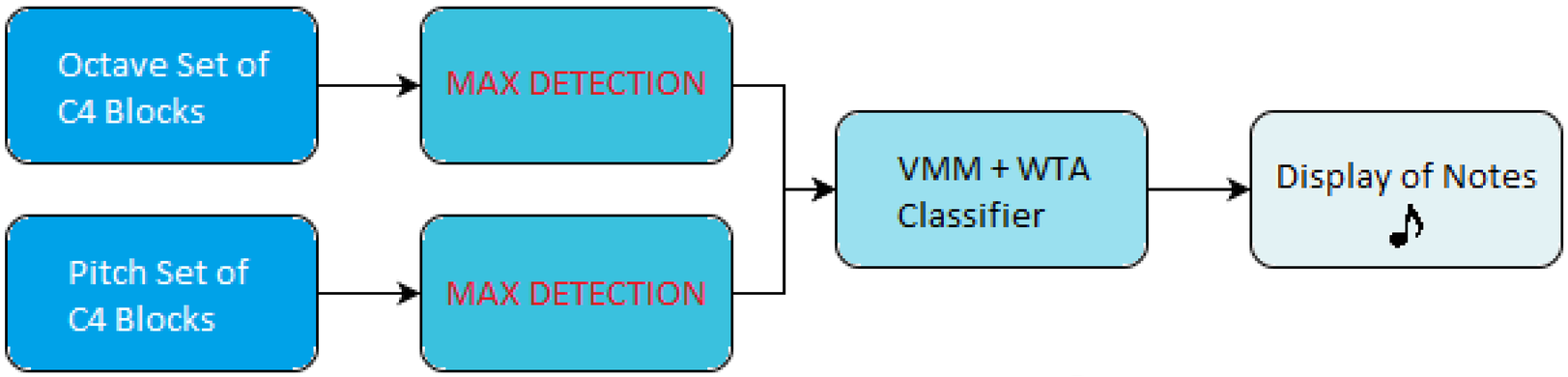

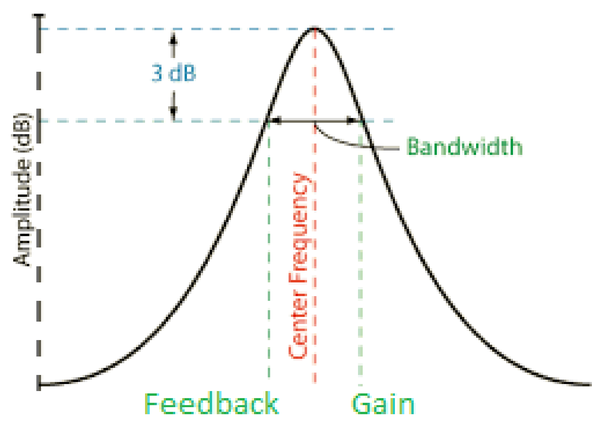

Steps:

FPAA Circuit Design:

- **Design two separate filter banks for separating different components of a sound for pitch detection**
  - **Octave filter bank**
  - **Tone filter bank**
- **Detect which filters within bank have the highest amplitude**
- **Classify the audio sample as a particular note based on amplitude patterns from filter bank**

Results:

- **Experimental data on relationship between feedback and gain biases of C4 filter**
- **Preliminary testing of numerous configurations of analog front end**

Future Work:

- **Improve quality factor and increase precision of filter bank**
- **Test amplitude detection and classification elements of circuit**
- **Display the classified notes on an Android application**

References:

[1] S. George, S. Kim, S. Shah, et. al, "A Programmable and Configurable Mixed-Mode FPAA SOC," IEEE Transactions on VLSI, 2016.

Add. Notes: Bode Plot image captured from *Waveforms* by Analog Discovery. Picture of sheet music found on Google Images.

Georgia Tech School of Electrical and Computer Engineering
College of Engineering

Sandia National Laboratories

7

Sensor System for Biomolecule Detection Using Flexible Sensor Array

Luca DeCicco, Leah Jackson, Katie Weatherwax, Mentor:Gunhee Kim Advisor: Dr. Kippelen
School of Electrical and Computer Engineering • Georgia Institute of Technology • Atlanta GA, 30332 USA

Opportunity Research Scholars' Program
School of Electrical and Computer Engineering
Georgia Institute of Technology

Georgia Tech Center for Organic Photonics and Electronics

Abstract

- Organic Field Effect Transistors (OFETs) have the potential to revolutionize the medical industry due to their flexibility, transparency, and low cost.
- Fabricated using organic semiconductors, these transistors will react to changes in biomolecule concentration.
- When integrated into a current reading circuit, these OFETs can collect medical data without the need for expensive and invasive tests.

Introduction

- Non-invasive and continuous monitoring improve medical diagnostics by using sweat, interstitial fluid or breath
- OFETs as biosensors have been used for a broad range of biodetection, including detection of pH, biotin, DNA, and drug delivery
- Previous challenges include aqueous conditions eroding the electrical characteristics

Background

Bottom Gate FET Structure

Dielectric Bilayer

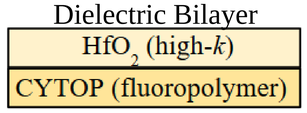

Environmentally stable gate

Semiconductor Layer

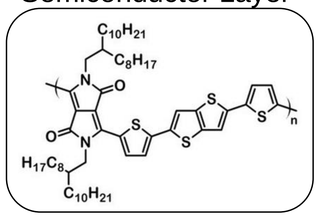

DPP-DTT: organic, high mobility hole transporting material

Experiment

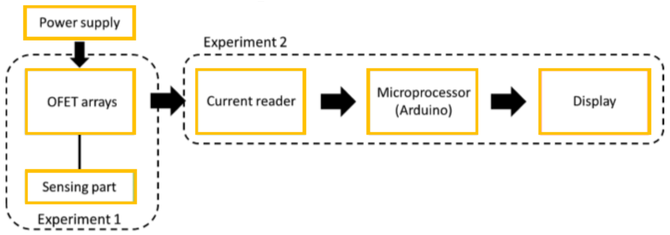

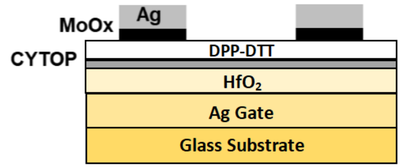

Experiment 1

- Fabrication of stable OFET arrays

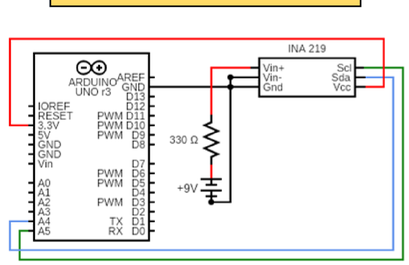

Experiment 2

- INA 219 reading the current across a resistor

Results

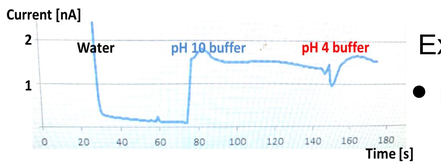

Experiment 1

- pH detection result using fabricated OFETs

Bus Voltage	1.03 V
Current	25.90 mA
Power	26.8 mW
Shunt Voltage	2.59 mV

Experiment 2

- Current across a 330 ohm resistor displayed on LCD screen

Discussion

- While fabrication is important, the system to implement the wearable sensor is critical.
- The intricacies of working with OFETs involve heat sensitivity, material availability, measurement limitations, and the small size.

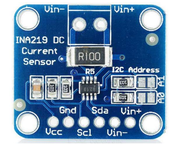

Future Work

- Print the OFETS on a flexible substrate.
- Test the entire device with an organic solution.
- Streamline the device for wearability.

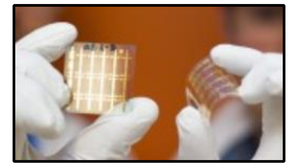

References

Vidor, Fábio & Meyers, Thorsten & Hilleringmann, U.. (2015). Flexible Electronics: Integration Processes for Organic and Inorganic Semiconductor-Based Thin-Film Transistors. Electronics. 4. 480-506. 10.3390/electronics4030480.
INA 219 Sensor Image: www.dx.com
Conductive Paint Image: https://www.amazon.com/Board-Li-Conductive-Adhesive-Flexible/dp/B07QKQYWMM
DPP-DTT Image: https://www.ossila.com/products/dpp-dtt-polymer?variant=30366225367136

Georgia Tech School of Electrical and Computer Engineering
College of Engineering

Texas Instruments

8

ORS
Opportunity Research Scholars' Program
School of Electrical and Computer Engineering
Georgia Institute of Technology

The Haiti RELAY Project: Empowering Haiti with Affordable Energy

Carah Camron, Amadou Diallo, Kevin Liow
Graduate Mentor: Kartavya Agarwal | Faculty Advisor: Deepak Divan

Texas Instruments

Motivation

Haiti is a Caribbean country that has been affected by natural disasters, corrupt government, and lack of infrastructure. The majority of the population still has limited access to the electricity, which means that even the most basic modern technologies are not available to them.

Project Goals

- Develop a compact, portable, & easy-to-use product to power small electronics & lighting
- Maintain sustainability of RELAY
- Replace Sealed Lead Acid Battery (SLAB) w/ Lithium Ion battery(Li+)

Previous Work

- Haiti RELAY
  - SLAB
  - 2 USB ports Output
    - 5 hours of house lighting
    - 2 full cell phone charges
- Distributed over 20 RELAYs in the past year to Haitian Entrepreneurs
- Sustainability of the RELAY is the team's priority

Previous RELAYs in the Field

System Design

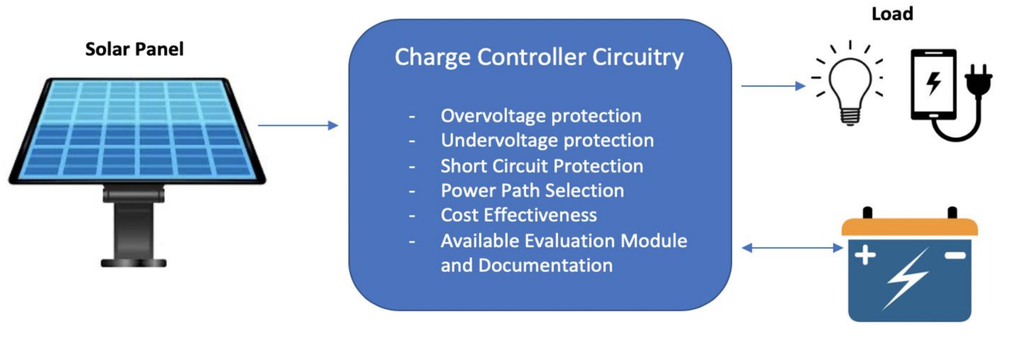

Proposed Soiar Home System Architecture

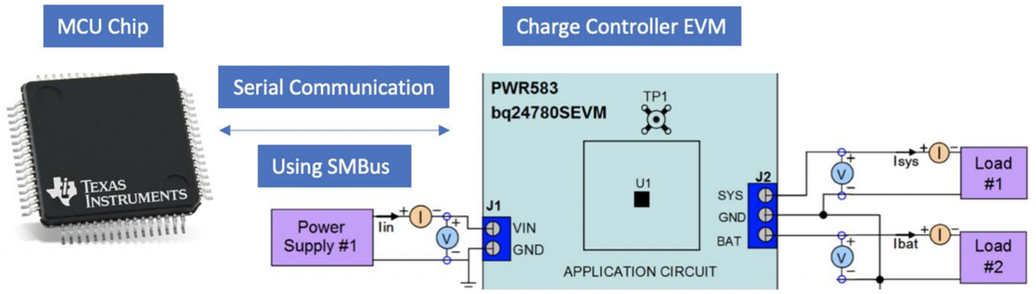

Detailed Design of Charge Controller Circuitry

Experimental Testing

- Targets: Ensure that the chosen IC bq24780s, meets System Requirements
  - Tested EVM using computer & SMBus to manually change registers
  - Tested EVM with DC Power Supply & Lithium Ion Batteries
  - Tested EVM with solar panel and light bulb output

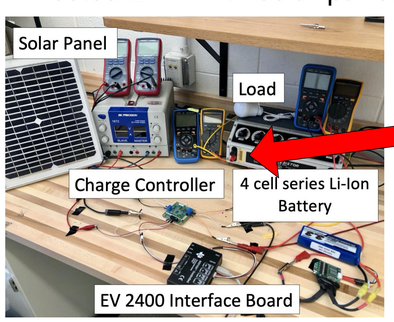

Experimental Setup

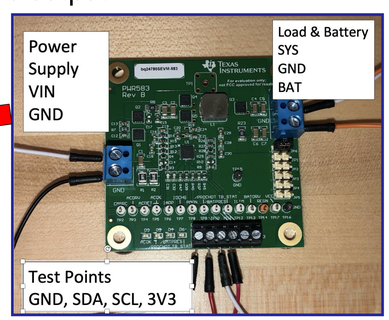

Close Up Of System Architecture

Experimental Results

- Set constant charge I & V
- Discharged/Charged Li+ within 10% of desired thresholds
- Controlled power path selection depending on available sunlight
- Charged phone battery and powered LED bulb
- Unable to provide enough power to EVM w/ solar panel

Conclusion

- The chosen IC meets all hardware requirements; however, a microcontroller (MCU) is needed so that the charge controller will function on its own.
- Acquired technical support guide from Texas Instruments to complete MCU architecture
- The IC, MCU, and Li-Ion batteries will raise upfront cost at least ~$20; however last at least ~2x longer

Future Work

- Complete software development & testing of MCU
- Design PCB and mechanical enclosure for deployment in Haiti
- Complete exhaustive testing of system for deployment
- Incorporate Pay As You Go (PAYGO) functionality via low-cost communications platforms enabled by bluetooth and 3G to reduce upfront cost

9

ORS
Opportunity Research Scholars' Program
School of Electrical and Computer Engineering
Georgia Institute of Technology

Optimizing Processor and Memory Peripheral Circuits Utilizing Computational Algorithms

Kenneth Holder, Jongheon Park, Mohamad-Baasim Rehan, Michael Schmidt, Mufutau Akuruyejo
{kholder9, jpark802, mrehan3, mschmidt, makuruyejo3}@gatech.edu

Nanoelectronics Research Laboratory
Dr. Azad Naeemi

Introduction

As the complexity of circuit design increases, the number of parameters to be optimized also increases. To tackle the high computational requirement of optimizing numerous parameters, a subset of computational algorithm, namely genetic algorithm was used to optimize a sense amplifier and tertiary content addressable memory (TCAM) circuit design.

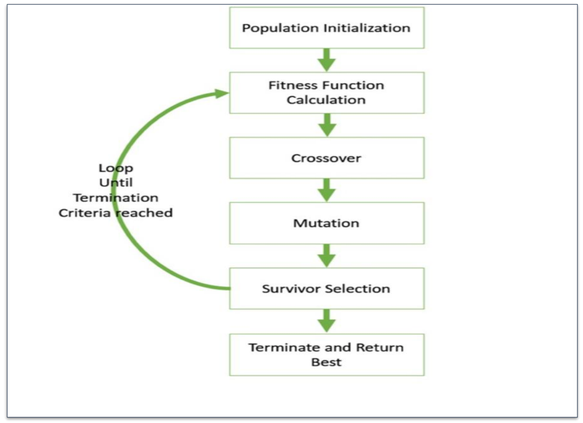

Fig. 1. Flow diagram of genetic algorithm

Background

Genetic algorithms are a subset of evolutionary computational algorithms that are inspired by the process of evolution in nature. It takes concepts from genetics such as random mutation, chromosomal crossover, and survival of the fittest to generate a solution to given parameters and constraints.

Methods

1. Literature Review
   - Review Genetic algorithms across various applications
   - Review the SPICE circuit simulator
2. Develop an Algorithm for Circuits
   - Create a genetic algorithm specifically for TCAM circuit and sense amplifier
3. SPICE Simulation and Testing
   - Run the algorithm and collect metrics measuring area, energy, delay, and EDAP (Energy, Delay, Area Product)
4. Successful Outcomes
   - Confirm that generated circuit matches the functionality of the existing one, and evaluate where improvements occur

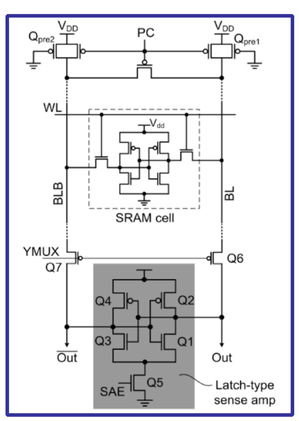

Fig. 2. Sense Amplifier and SRAM to optimize

Sense Amplifier Results

- **Parameters changed:**
  - Different PN Ratio of inverters for the same sense amplifier
  - Beta Ratio Maximizes at 4.0
  - Gamma Ratio: Reached constant value
- **Metrics being measured:** Read Time/Energy, EDP, Area, EADP
- All metrics decreased after optimization

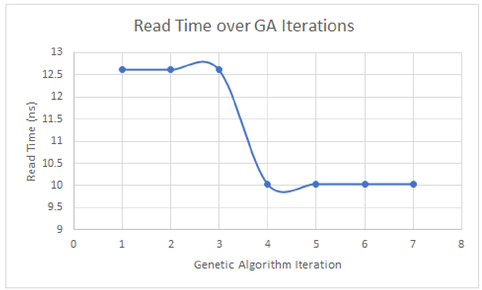

Fig. 3. History of read time through generation

TCAM Results

- Optimized for best EDAP output
- Decreased area and energy but increased delay

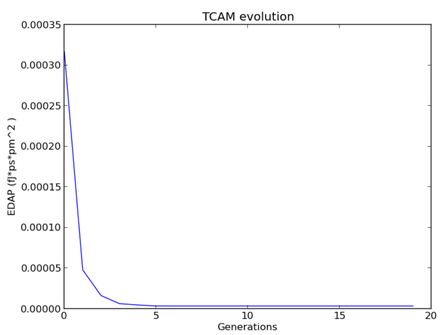

Fig. 4 History of best EDAP through generations

Conclusions

Genetic algorithms provided the optimal set of circuit parameters for optimized functionality:

- Some parameters provide greater variation in desired results
- Power supply parameters provide greater effect than transistor size

Future Work

- Vary connections in the circuit and rearrange components to provide even better metrics and create full new topologies
- Explore the use of genetic algorithms into other analog circuits outside of memory

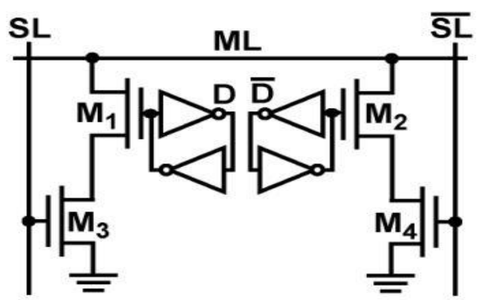

Fig. 4. 16T TCAM

Georgia Tech School of Electrical and Computer Engineering
College of Engineering

Acknowledgements: Dr. Azad Naeemi

10

Opportunity Research Scholars' Program

School of Electrical and Computer Engineering
Georgia Institute of Technology

An Investigation of Micromotor Technology Enabling Mechanically Reconfigurable Reflectarrays

Alessandria Holley, Nathan Jenkins, Saiharshith Kilaru, Chandler Mason, Maria Saito
PhD Mentor: Joshua Roper | Faculty Advisor: Dr. Andrew Peterson

Viasat

Background

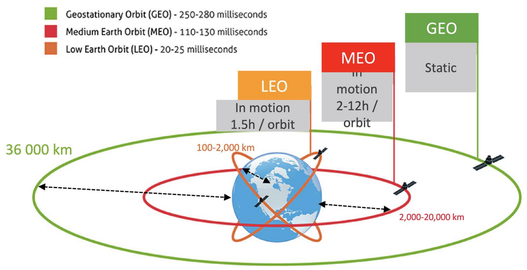

Figure 1:Figure explaining different satellites [1]

- Low Earth Orbiting satellites (LEOs) provide low-latency internet
- Antennas used to communicate with LEOs are cost-prohibitive for consumer use
- Objective is to create a more affordable antenna array that is accessible to the average consumer
- Proper array phase synthesis and spatial phase delay at the element level must be calculated to determine the angle to move the elements in the array
- Phase delay equation:

$$k_0(R_i - \bar{r}_i \cdot \hat{r}) - \psi_i = 2\pi N$$
$$\varphi_{spd} + \varphi_{ppd} = 2\pi N$$

- Spatial phase delay equation:

$$\varphi_{spd} = k_0 R_i$$

Project Goal

- Create 10 element by 10 element array
- Each element to be individually configurable
- Elements to be controlled by a central computer that can constantly determine new desired angle of elements and can drive motors to change angle

Procedure

- Create four prototype 2x2 element arrays
- Determine prototype design to expand to 10x10
  - For hardware setup, look at various combinations (shown left) of microcontroller and motor
  - Decipher pros and cons regarding efficiency and cost
  - Select the best combination
- Build upon the combination and develop 10x10 prototype

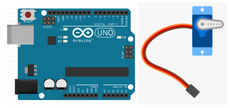

Figure 3: Arduino Uno & Servos.
Source: [6] [9]

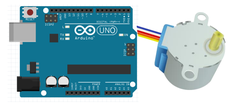

Figure 4: Arduino Uno & Steppers.
Source: [6] [7]

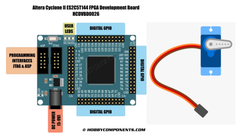

Figure 5: Altera Cyclone II & Servos.
Source: [8] [9]

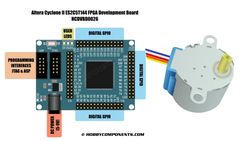

Figure 6: Altera Cyclone II & Steppers.
Source: [8] [7]

Architecture

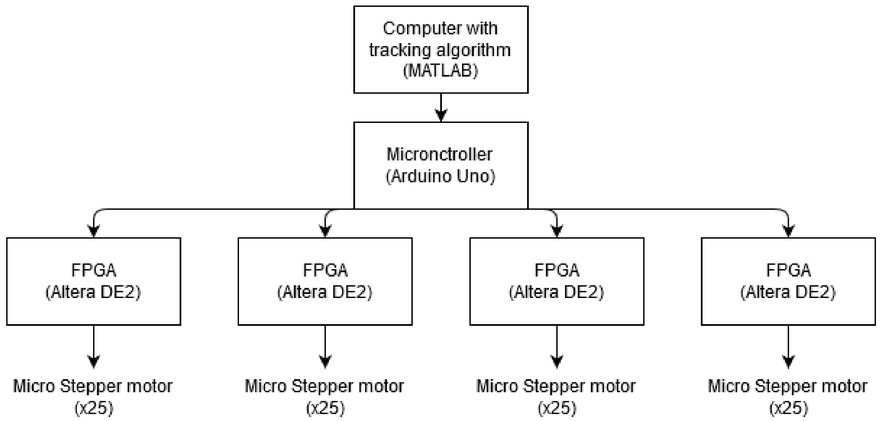

Software

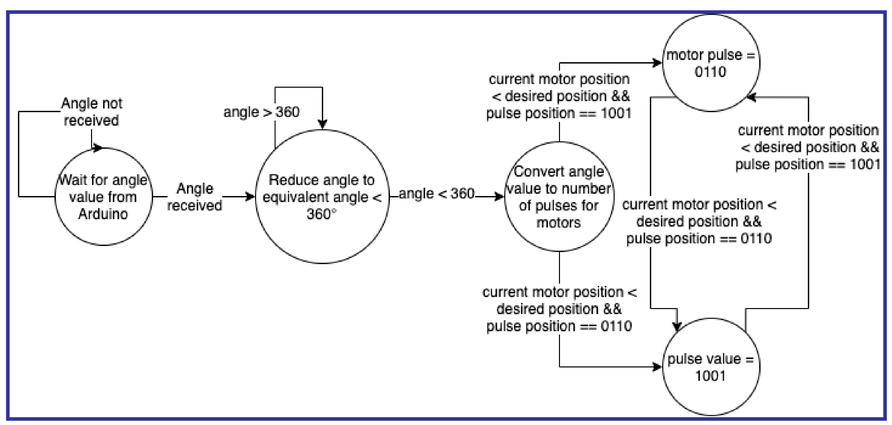

- 1 FPGA controls a quadrant (25 elements) of array
- 1 Arduino sends angles from MATLAB script to FPGAs

Current Status

- Working on the SPI protocol, which is how the FPGA will communicate with each other and the arduinos.
- Physical assembly in progress: milled antenna elements, soldered motors and motor drivers

Future Work

- Continue building up to 10 x 10 array
- Getting real time input and computation to work
- Fully assemble motor fixture
- Create custom PCB to further decrease cost

Acknowledgments

[1] Hurst, N. (2019). Types of Satellites. [image] Available at: https://www.pcmag.com/article/362695/why-satellite-internet-is-the-new-space-race [Accessed 22 Oct. 2019].

[2] Manohar R, Sophiya Susan S, "Radiation Analysis of Phased Antenna Arrays with Differentially Feeding Networks Towards Better Directivity" IRJET, Vol. 05, Issue 04, pp. 3586-3590, April 2017.

[3] X. Yang, "A broadband high-efficiency reconfigurable reflectarray antenna using mechanically rotational elements," IEEE Trans. Antennas Propag., vol. 65, no. 8, pp. 3959–3966, Aug. 2017.

[4] "Stepper vs Servo" Available at: https://www.amci.com/industrial-automation-resources/plc-automation-tutorials/stepper-vs-servo/

[5] Iyer, Rahul. "FPGA Tutorial: Intro to FPGAs with the Mojo – Part 1," Available at: https://www.deviceplus.com/how-tos/fpga-tutorial-intro-to-fpgas-with-the-mojo-part-1/

[6] L293D. "Arduino UNO." *Wikimedia*, 21 Nov. 2017, commons.wikimedia.org/wiki/File:Arduino_uno.png.

[7] Irenaklein9. "Stepper Motor Electric Motor PNG." IMGBIN, 23 Dec. 2018, imgbin.com/png/8yh8dLWu/stepper-motor-electric-motor-png.

[8] "Altera Cyclone II ES2C5T144 FPGA Development Board HCDVBD0026." Hobby Components, hobbycomponents.com/images/forum/Altera_Cyclone_II_Diagram.png.

[9] "Servo Motor Clipart." *King PNG*, www.kindpng.com/picc/m/99-996706_servo-motor-clipart-hd-png-download.png.

Georgia Tech School of Electrical and Computer Engineering
College of Engineering

11

ORS
Opportunity Research Scholars' Program
School of Electrical and Computer Engineering
Georgia Institute of Technology

Georgia Tech Machine Learning

Spectral Optimization Via Discrete Prolate Spheroidal Sequences

Juan Antonio Elizondo-Villasis, Siddhanta Panda, Vijay Nilesh Prasad,
Mentor: Coleman DeLude, Faculty Advisor: Dr. Justin Romberg

SCHOOL OF ELECTRICAL AND COMPUTER ENGINEERING · GEORGIA INSTITUTE OF TECHNOLOGY

TTM Technologies

Background

- Classical signal processing has centered around Fourier analysis
- Introduces the time-frequency concentration problem → a signal cannot have finite support in both time and frequency domains
- Discrete prolate spheroidal sequences (DPSS or "Slepian" sequences) provide an efficient representation for discrete signals that are maximally concentrated in time and frequency

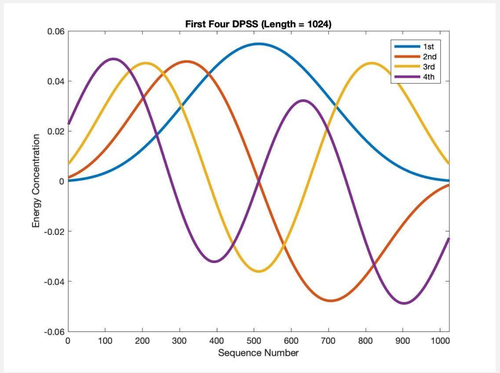

Figure 1. First four DPSS of length 1024 where the first sequence maximizes the ratio of energy contained in the band [–W,W].

Objectives

- To apply Slepian-based techniques to classical problems typically addressed in the Fourier domain
  - Spatial filtering (beamforming) → Utilization of sensor array data to spatially filter signals
  - *Sleptograms* → Slepian domain equivalents to Fourier domain spectrograms, visual display of frequency spectrum

Beamforming

- MATLAB simulation of a 64-element antenna array
- Create sinusoidal modulation vectors that fire five beams from five different incident angles
- Project modulation vectors onto the Slepian basis
- Separately, project modulation vectors onto the Fourier basis
- Plot the respective power spectra
- Observe that Slepian-based beam is wider than Fourier-based beam with lower sidelobes

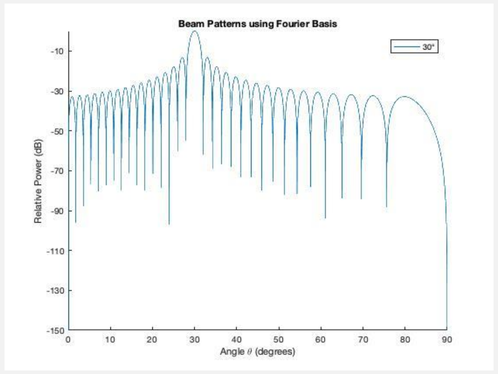

Figure 2. Fourier-based beam centered at 30°.

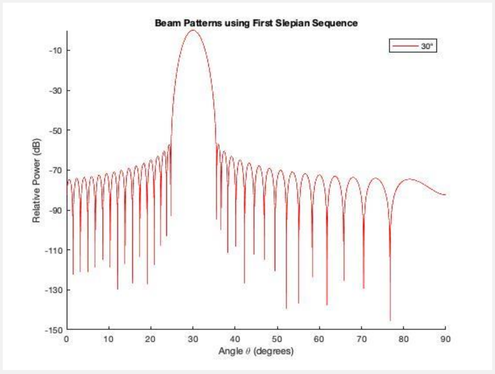

Figure 3. Slepian-based beam centered at 30°.

Sleptograms

- Signal of interest is a sum of 1000 sinusoids
- Observe that Slepian basis lowers sidelobes compared to Fourier basis (traditional spectrogram)
- Multitaper results in higher sidelobes, but smooths out the frequency spectrum by using the first *2NW* Slepian basis vectors to estimate the power spectrum of the signal where *N* is the signal length and *W* is bandwidth of 20 Hz

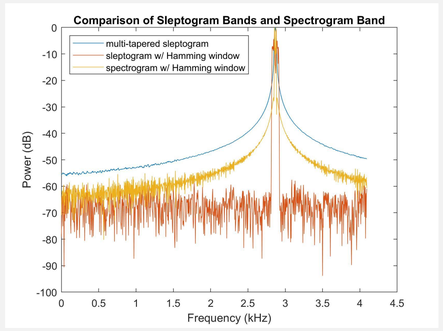

Figure 4. Power spectrum comparing Fourier, Slepian, and multitapered windows. Using a Hamming window also reduces spectral leakage.

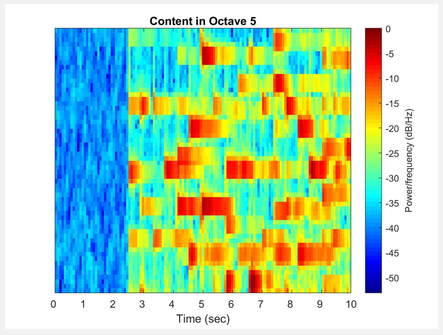

Figure 5. *Sleptogram* sample of Pachelbel's "Canon in D". Compared to a Fourier-based spectrogram, the relative power per frequency band is higher.

References

[1] Karnik, S., Zhu, Z., Wakin, M., Romberg, J. and Davenport, M. (2019). The fast Slepian transform. Applied and Computational Harmonic Analysis, 46(3), pp.624-652.

[2] Wang, L. (2017). A Review of Prolate Spheroidal Wave Functions from the Perspective of Spectral Methods. Journal of Mathematical Study, 50(2), pp.101-143.

12

Exploring Fabrication of Thin-Layered TMD Solar Cells

Hubert Elly, Shashwati da Cunha, Yi Li, William Schaffer
Advised by: Dr. Minkyu Cho, Dr. Shyh-Chiang Shen
School of Electrical and Computer Engineering • Georgia Institute of Technology

ORS Opportunity Research Scholars' Program
School of Electrical and Computer Engineering
Georgia Institute of Technology

Semiconductor Research Laboratory GeorgiaTech

Abstract

We investigate the possibility of fabricating MoS_2 to (p)-Si heterojunction solar cells via spin coating. Conventional methods of fabrication involve intricate and expensive processes such as chemical vapor deposition (CVD). If achievable, spin coating would provide a cheap and low-resource method for TMD solar cell fabrication.

Introduction

Silicon solar cells can reach a conversion efficiency of 30%, but these cells come at a high cost. TMD materials can be made into few layers that are only nanometers thick and still maintain high photon absorption rate. These layers show high efficiency for many possible applications.

Background

By utilizing poly-silicon, commercially used solar cells typically reach a conversion rate of 15-20%. The application of solar cells range from everyday residential use to outer space satellite power supply but are restricted by its cost. The main factors that make photovoltaics expensive are limited efficiency, material constraints, and manufacturing costs.

Experimental Procedure

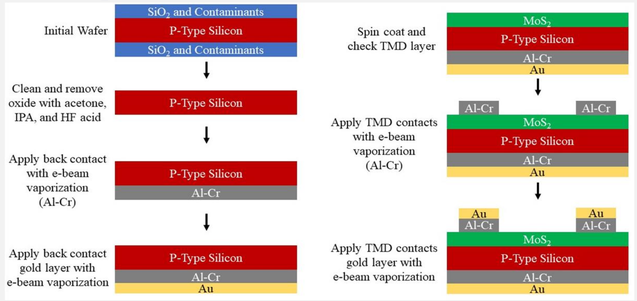

Spin coating protocol:

- 1 mg/mL solution
- 3000 rev/min
- 60 sec duration
- Room temperature
- Wafer dried on 120°C hot plate
- Repeated to coat multiple layers

Results

SiO_2 of Thickness 6,400 Å

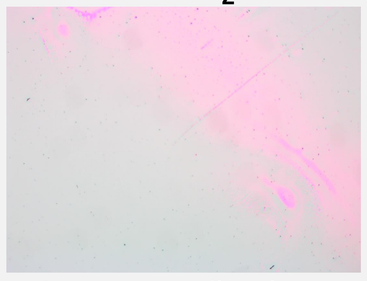

2 TMD Applications

No Applications

Samples were successfully coated with MoS_2. However, the resulting film needs to be made uniform, and its thickness is yet to be characterized.

Future Work

Our current model can be improved upon by using theoretical models to optimize various parameters, such as the silicon doping concentration, the number of MoS_2 layers, and the tensile strain of the materials, to achieve maximum quantum efficiency. However, they are still being explored.

TMD Characterization Methods

- Raman spectroscopy measures the number of atomic layers and film thickness.
- Scanning electron microscopy (SEM) is a visual method to study film uniformity.

TMD Solar Cell Analysis

IV curve measures the electrical response under different conditions:

- Dark Condition Photocurrent
- Under Illumination

References

1. , "Two-dimensional transition metal dichalcogenide-based counter electrodes for dye-sensitized solar cells," RSC Advances, vol. 7, no. 45, pp. 28234–28290, 2017.
2. "Lateral and vertical heterostructures in two-dimensional transition-metal dichalcogenides". Opt. Mater. Express, 9, pp. 1590-1607, 2019.
3. https://www.nature.com/articles/s41586-018-0574-4#Sec2

Georgia Tech School of Electrical and Computer Engineering
College of Engineering

SRC Semiconductor Research Corporation

13

ORS
Opportunity Research Scholars' Program
School of Electrical and Computer Engineering
Georgia Institute of Technology

High Resolution Imaging and Object Detection for NASA's JunoCam

Alison Kennedy, Caleb Page, Gracen Wallace, Cory Wang, Amoree Hodges
{akennedy43, cpage34, gwallace30, cwang681, ahodges}@gatech.edu

Planetary Atmospheres Lab
Dr. Paul Steffes

Introduction

NASA's Jupiter Satellite, Juno, has a visible light camera, Juno Cam, that is aimed at public outreach.

Our team is creating image enhancing algorithms to provide higher quality satellite images to the scientific and image processing communities.

Data Set

This year, we acquired images from the Juno Cam's public website.

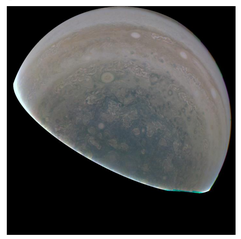

Now we are stitching, color correcting, and creating a dataset of our own Juno Cam Images through:

- ISIS3
- Photoshop

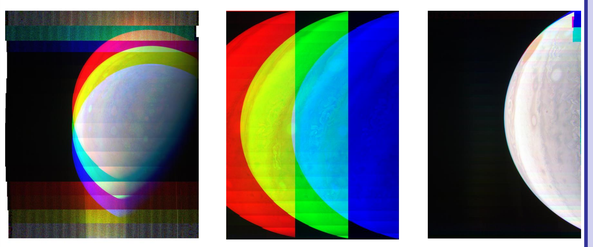

Snapshots of the Color Correction Process.

High Resolution

Deconvolution

Image Restoration methods to aid Super Resolution Algorithm.

- Weiner Filter: Produces an image with a minimized Point Spread Function (PSF)
- Lucy Richardson (LR): Attempts deconvolution without knowing the PSF. User inputs "guess" of PSF and recursive algorithm improves this "guess".

Super Resolution

Machine learning to improve image resolution by estimating missing pixels

- Trained with DIV 2K dataset
- Layers: 2D Convolution, Activation (RELU), Regression (MSE)

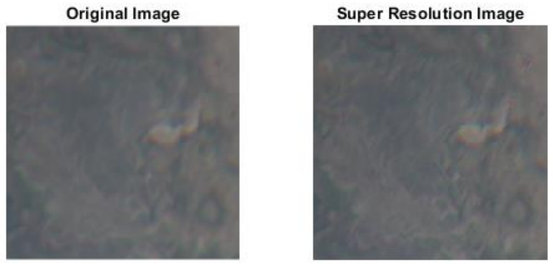

Satellite image before and after being input into super resolution network

Object Detection

Template Matching

Algorithm:

- Convert inputs into grayscale
- Calculate mean intensities
- Subtract out mean intensities
- Flip the template image
- Convolve for final output

Convolutional Network

- To identify objects on Jupiter's surface using TensorFlow 2.0 and Keras
- Beginning with a preexisting dataset to develop an initial network (CIFAR-10)
- Layers: 2D Convolution, Max Pooling, Dense, RELU, Flatten

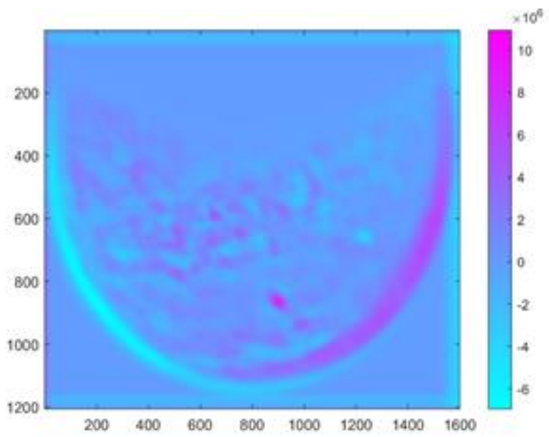

Template matching output, showing identified object at the dark purple spot

Results

- MATLAB implementations of Weiner Filter and LR produced mean squared errors of 0.0037 and 0.0197, respectively.
- ConvNet dataset produced a training accuracy of 96% and validation accuracy of 70%

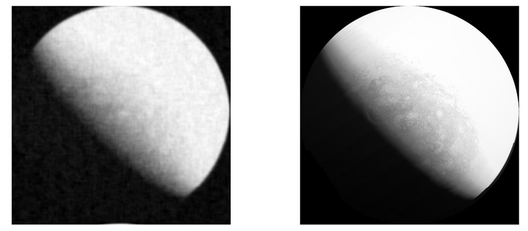

Results of deconvolution with Weiner and LR

Future Work

- Creating Juno dataset for neural network training
- Improve Lucy Richardson with Monte Carlo experiments
- Developing unsupervised super resolution neural network
- Testing ConvNet to detect if objects are present in an image (Red spot, String of Pearls)

Georgia Tech School of Electrical and Computer Engineering
College of Engineering

Viasat

Acknowledgements: Thank you to Viasat, Dr. Paul Steffes, Amoree Hodges, and the Juno Science Team

14 ORS
Opportunity Research Scholars' Program
School of Electrical and Computer Engineering
Georgia Institute of Technology

Inverse Design of Electronics using Machine Learning

Vinay Balamourougan, Eunsan Mo, Jessica Graham, Majid Ahadi Dolatsara, Madhavan Swaminathan

School of Electrical and Computer Engineering, 3D Systems Packaging Research Center (PRC), Georgia Institute of Technology, Atlanta GA, 30332 USA

Abstract

- Our goal is to inversely design a circuit. We approached this with linear /polynomial regression and neural networks.
- Out of the three methods the results were most accurate with Linear Regression.
- Polynomial regression and neural networks require around 100 data points to work.

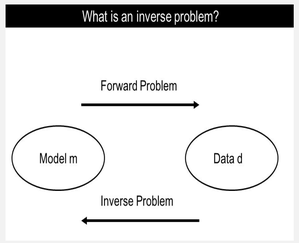

Introduction

- Our goal is to reduce the amount of effort and time it takes to design a complex circuit.
- Given a desired output, the algorithm should be able to use inverse design to specify the values of the parameters in the circuit.

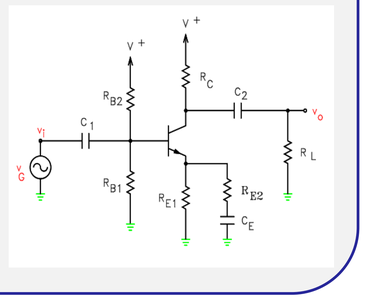

Background

- We investigated different machine learning algorithms:
- Neural Networks:
  - Typically effective in modeling non-linear relationships and commonly used to predict:
    - Microwave filters and predicting nanoparticle
- Polynomial and Linear Regression:
  - Used with inverse design of microwave circuits

Experiment

- Predict resistor values of an amplifier circuit based on gain using the following machine learning algorithms
  - 1. Linear Regression
  - 2. Polynomial Regression
  - 3. Neural Networks
- For each algorithm, the amplifier was modeled for the forward pass
  - Gain predicted based off values from 6 resistors as they impact gain
- Inverse design used 4 voltages and 4 currents to predict the 6 resistances.

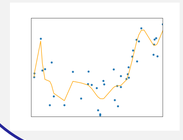

Forward Pass

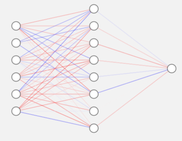

Inverse Design

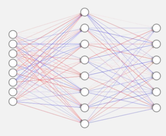

Results

For Linear Regression

Euclidian norm = 0.3001

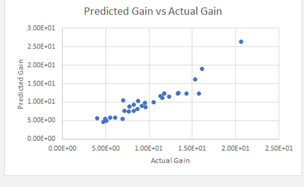

For Polynomial Regression

Euclidian norm = 0.5993

For the Neural Network

Euclidian norm = 0.5136

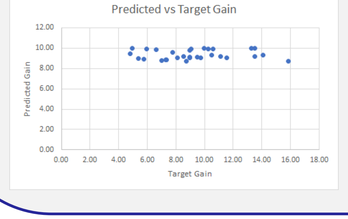

Euclidian Norm Formula: $\frac{\sqrt{\sum e_i^2}}{N}$

Discussion

- Each machine learning algorithms requires eight inputs from the user. It is inconvenient to calculate four different voltages and currents.
- In the future we can train the algorithm to take one input from the user and make an educated guess about the seven other inputs to pump out an output.

Conclusions

- Our research focuses on the application of neural networks and polynomial/linear regression algorithms to the inverse design problem.
- In our results we concluded that we could predict the parameters with a varying level of accuracy.
- The next step would be to:
  - Make a GUI interface for the user.
  - Train the algorithm to make an educated guess about the unknown inputs.

References

K. Roy, M. Ahadi Dolatsara, H. M. Torun, R. Trinchero, and M. Swaminathan, "Inverse Design of Transmission Lines with Deep Learning." in *IEEE Electrical Design of Advanced Packaging and Systems Symposium (EDAPS)*, pp.1–2.

I. Elshafiey, L. Udpa, and S. S. Udpa, "Application of neural networks to inverse problems in electromagnetics," IEEE transactions on magnetics, vol. 30, no. 5, pp. 3629-3632, 1994.

Georgia Tech School of Electrical and Computer Engineering
College of Engineering

Cooperative Exploration of Unknown Environments Using a Robotic Snake-Turtlebot Leader-Follower Pair

Alexander Faché, Sterling James, Kimberly Lie
PhD Mentor: Alex Chang, Faculty Advisor: Patricio Vela

School of Electrical and Computer Engineering
Georgia Institute of Technology

Problem

Evaluation/validation of novel robotic snake locomotive planning and exploration frameworks are limited by physical constraints (e.g. tethers, battery capacity, compute power.

In research settings, experimental evaluation of snake-like robotic locomotion strategies can benefit tremendously from an ability to travel un-prohibited over large expanses of terrain. In order to realize such a capability, we adapt a Turtlebot to act as a 'follower' command center providing instructions, power, and computation.

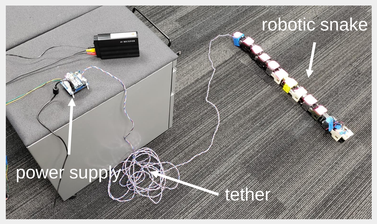

Previous implementations prohibited free movement by snake-like robots.

Leader-Follower Pair

- **Robotic Snake** (*leader*)
  - 10 Dynamixel motors
  - 3D-printed scales provide locomotive friction
  - *Tether* provides power and motor commands
- **Turtlebot** (*follower*)
  - Differential drive vehicle
  - *Robotic snake tracking*: Logitech C920 / Intel RealSense D435i cameras
  - Supplies power and commands to robotic snake

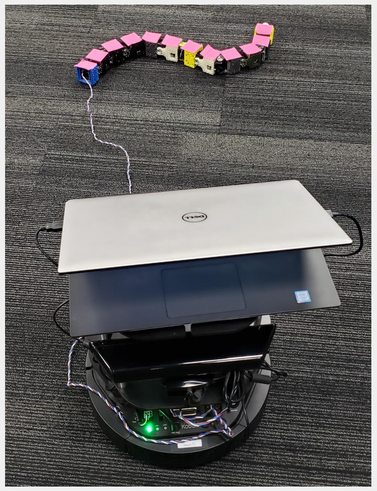

*Robotic snake (**top**) and Turtlebot (**bottom**)*

Leader-Follower Architecture

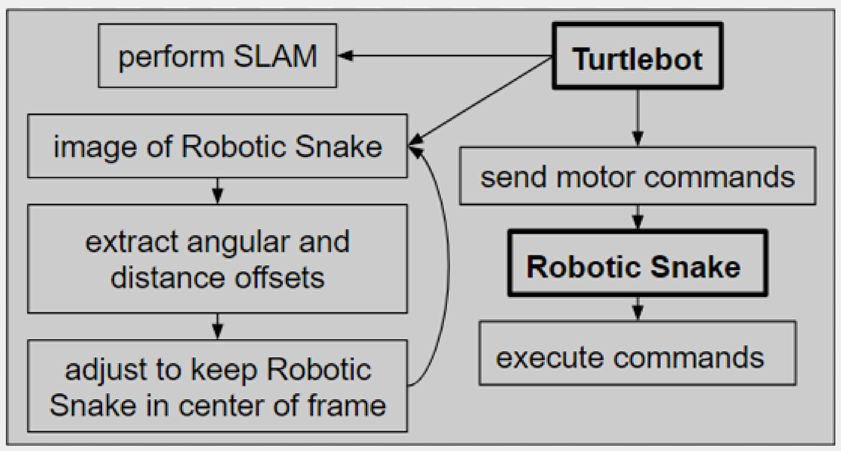

Robotic Snake Motion

- Robotic snake travels using different motion primitives

Sidewinding

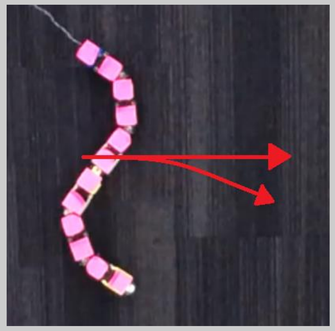

- Robot ***translates laterally*** using a motion, mimicking bipedal motion
- Changes in the curvature of the 'average body' adjusts how straight the robotic snake travels
- Most locomotively efficient gait

Turn-in-Place

- Two part gait cycle
  - Ends lift, body curls up
  - Ends drop, body straightens
- Accomplishes both ***clockwise*** and ***counterclockwise rotation***
- Minimal translation occurs

- Modulating parameters (e.g. amplitude, frequency) allows control of overall time-averaged gait motion

Turtlebot: Tracking / Planning

- Tracking of robotic snake
  - *Objective*: Keep robotic snake in center of Turtlebot camera frame and maintain a specified distance
  - Magenta markers placed on robotic snake

Robotic snake with magenta markers

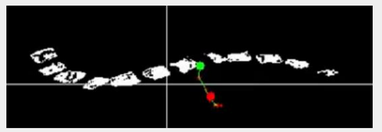

Markers segmented from environment

- Open Motion Planning Library (OMPL)
  - Used to plan paths for both Turtlebot and robotic snake between specified start and end positions

OMPL Environment

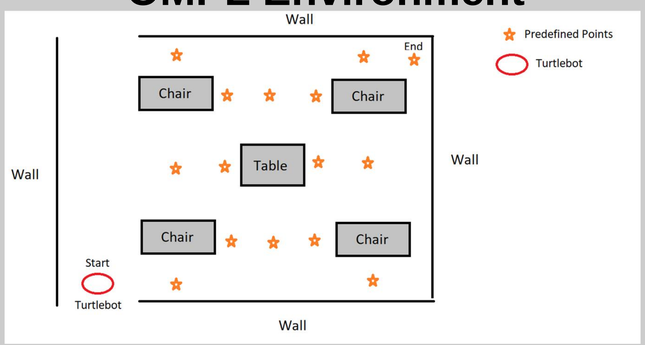

Leader-Follower Scenario

- Turtlebot tracks robotic snake that is executing sidewinding and turn-In-place motion primitives
  - Time proceeds from top-to-bottom

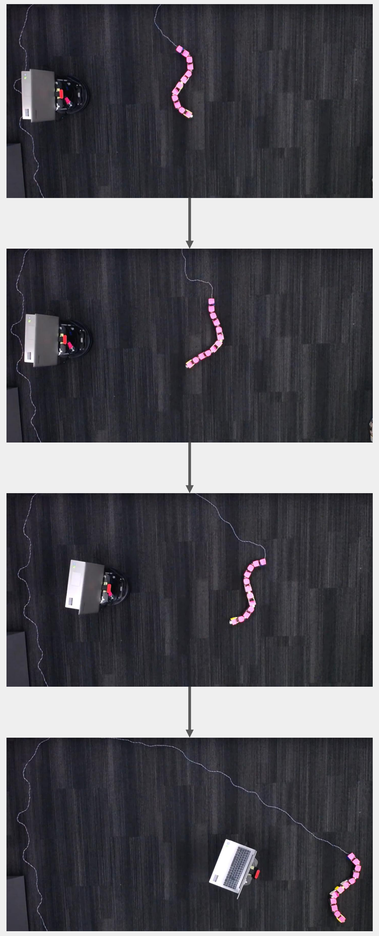

(1) *Initial position of Turtlebot and Robotic Snake.*

(2) *Robotic Snake is performing straight sidewinding with Turtlebot tracking.*

(3) *Continued command following and tracking.*

(4) *Final position.*

Conclusion

- Tracking system implemented: Turtlebot maintains robotic snake in center of view, following at specified distance
- Sidewinding motion controller implemented: Current robotic snake does not permit sufficient steering control

Future work

- Synthesize alternative sidewinding steering strategy
- Integrate tracking/following, planning, and gait control to accomplish Robotic Snake-Turtlebot leading/following

Georgia Tech School of Electrical and Computer Engineering
College of Engineering
Texas Instruments
NSF
IVALAB Intelligent Vision and Automation Laboratory

17

Opportunity Research Scholars' Program

School of Electrical and Computer Engineering
Georgia Institute of Technology

A Robust Learning-Based Motion Planner for Navigating an Unknown Environment

IVALAB
Intelligent Vision and Automation Laboratory

Brennon Farmer, Dylan Nektalov, Tara Poteat, Rajan Vivek, PhD Mentor: Shiyu Feng, Faculty Advisor: Dr. Patricio Vela

School of Electrical and Computer Engineering • Georgia Institute of Technology • Atlanta GA, 30332 USA

Introduction

- The volatility of real-world environments limits the success and versatility of existing motion planners for autonomous navigation.
- **Supervised learning** using expert demonstrations from existing planners can be used to map directly from sensor data and target location to steering commands.
- A **deep neural network (DNN)** trained using a non-learned motion planner can output effective steering commands to a target in **unknown environments.**
- **Greater robustness** (noise immunity and applicability to various robot geometries) should be attainable by DNN using varied training data.

Background

- **Traditional Hierarchical Planner:**
  - **Global Planner**: Uses preloaded map to generate collision-free path
  - **Local Planner**: Uses sensors to avoid obstacles not anticipated by global planner
- **Dynamic Window Approach (DWA):** Non-learned algorithm for local planner
- **Neural Network**: Uses a network of functions to understand and translate a data input (features) of one form into a desired output

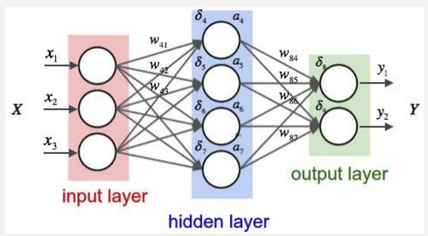

Figure 1. A simple fully-connected neural network. Each neuron connection is assigned a weight (w). The hidden layer translates the inputs (X) to an output (Y) through a function. The weights are learned through backpropagation (involving δ) by minimizing the error between the desired output and the actual output.

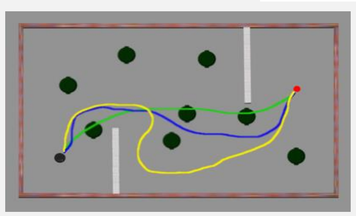

Figure 2. Paths generated by a global planner (green) and a local planner (yellow). The blue path represents the optimal path.

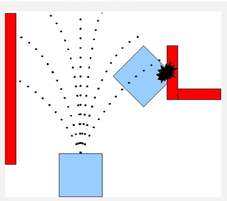

Figure 3. A robot using the DWA algorithm. The robot's velocity is sampled. Forward simulations based on the velocity are performed from the robot's current state. They are evaluated with a metric penalizing for proximity to obstacles and rewarding for proximity to global path. The best velocity is chosen.

Methods

Data Collection (Inputs to Network)

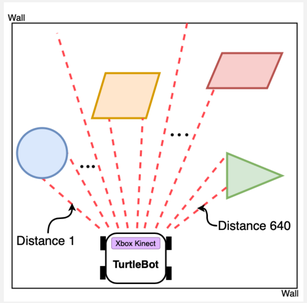

Figure 4. Laser scan data for the TurtleBot. The TurtleBot collects distances (in meters) to the closet obstacles detected.

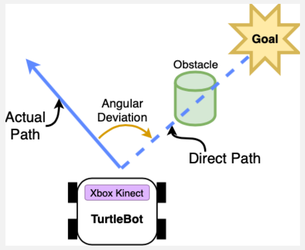

Figure 5. Angular deviation (in radians) of the TurtleBot's direction from the straight-line path to the goal.

	Time	Distance to Goal	Ang Dev (straight line to goal)	Forward(0), Left(1), or Right(2)	Distance 1	Distance 2	Distance 3	Distance 4	Distance 5	Distance 6
0	45	3.4	-1.0	0	4.2	4.2	4.2	4.2	4.2	4.2
1	45	3.4	-1.0	2	4.2	4.2	4.2	4.2	4.2	4.2
2	45	3.4	-1.0	2	4.2	4.2	4.2	4.2	4.2	4.2
3	45	3.4	-0.9	2	4.2	4.2	4.2	4.2	4.2	4.2

Figure 6. Small sample of the data collected using the Turtlebot. The distances and angular deviation are then used as inputs for the neural network, while the directions are used as expert outputs.

Steps Performed

1. Collect sensor data using ROS Gazebo simulation.
   a. Robot randomly assigned starting position and goal
   b. Robot navigates with DWA
2. Categorize robot trajectory to be forward, left, or right.
3. Design a deep neural network that uses the set of distance data and straight line angular deviation as inputs and outputs the direction of travel.
4. Train the DNN, minimizing the difference between its output and the expert output from step 2.
5. Adjust hyperparameters and network structure.
6. Test DNN and repeat.

Overall Network Structure

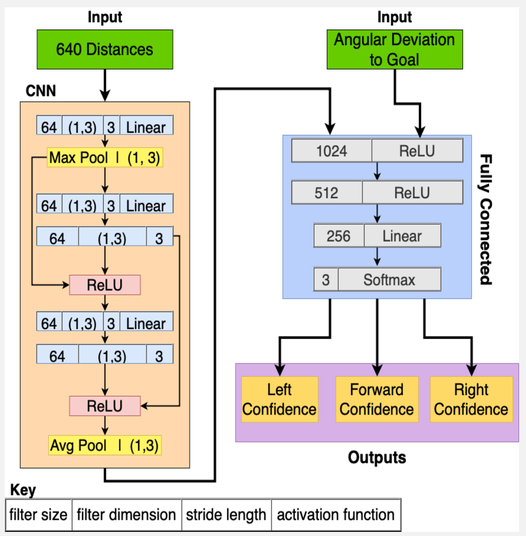

Figure 7. The Convolutional Neural Network (CNN) is used because it can recognize features that span multiple distance measurements. Pool layers are used to reduce overfitting. The CNN takes in the distance array and outputs to a fully connected neural network, where it is fused with angular deviation from the goal. The network then selects which direction the robot should travel in. Each output direction will only be followed by the robot for a fraction of a second, allowing the robot to make smooth turns.

Results

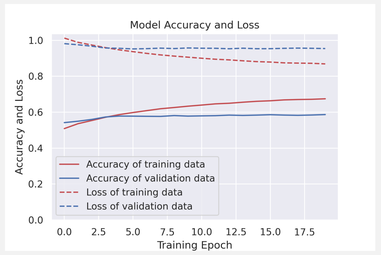

Figure 8. Graph shows the accuracy and loss of training and validation (unknown environment) data throughout the eight-hour training session.

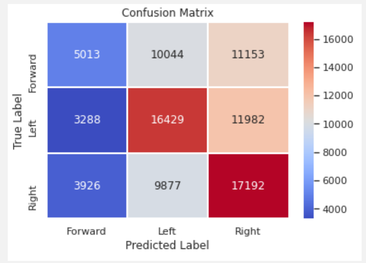

Figure 9. Confusion matrix compares the amount of samples of each direction category and the corresponding category assignment of the DNN. A high number in a square where the true label and predicted label do not match indicates confusion.

- DNN achieved an accuracy of 67% when outputting directions in seen environments and 58% in unknown environments
- DNN struggled to differentiate forward samples from left or right
- DNN was significantly more accurate at identifying right samples than other categories

Discussion / Future Work

- The results demonstrated that the **DNN could generalize its learning** from training data to navigate previously unseen environments.
- The DNN accuracy could be improved by **increasing training samples.**
- Using more varied training data such as other robot geometries, environments, or adding artificial noise to training data could **increase DNN robustness**.
- The DNN should be **evaluated on a real Turtlebot** in an unknown environment to compare its effectiveness to DWA and other non-learned motion planners.

References

[1] S. Levine, C. Finn, T. Darrell, and P. Abbeel, "End-to-end training of deep visuomotor policies," J. Mach. Learn. Res., vol. 17, no. 1, pp. 1334–1373, Jan. 2016. [Online]. Available: http://dl.acm.org/citation.cfm?id=2946645.2946684

[2] "Wiki," *ros.org*. [Online]. Available: http://wiki.ros.org/teb_local_planner. [Accessed: 06-Oct-2019].

[3] J. S. Smith, S. Feng, F. Lyu, and P. Vela, "Real-Time Egocentric Navigation Using 3D Sensing," in *Machine Vision and Navigation*, .

[4] "TensorFlow," *TensorFlow*. [Online]. Available: https://www.tensorflow.org/. [Accessed: 05-Oct-2019].

[5] N. Varas, "move_base," ros.org. [Online]. Available: http://wiki.ros.org/move_base. [Accessed: 05-Oct-2019].

[6] "Wiki," *ros.org*. [Online]. Available: http://wiki.ros.org/dwa_local_planner. [Accessed: 06-Oct-2019].

[7] M. Pfeiffer, M. Schaeuble, J. Nieto, R. Siegwart, and C. Cadena, "From perception to decision: A data-driven approach to end-to-end motion planning for autonomous ground robots," *2017 IEEE International Conference on Robotics and Automation (ICRA)*, 2017.

Georgia Tech School of Electrical and Computer Engineering
College of Engineering

intel

18

Opportunity Research Scholars' Program

School of Electrical and Computer Engineering
Georgia Institute of Technology

Convolutional Neural Networks in a Hardware Accelerator Design

Emerging Devices and Circuits Lab

Malik Burton, Mory Fode Traore, Laura Heller, Tarun Maddali

PhD Mentor: Xiaochen Peng Faculty Advisor: Dr. Shimeng Yu

Semiconductor Research Corporation

Motivation

Machine learning is a growing field and it is pushing limits of current hardware capabilities because Hardware needs to keep up with machine learning

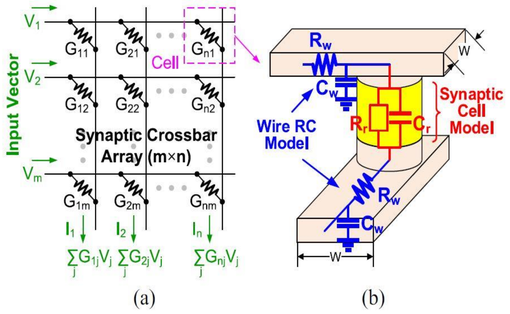

Figure 1: (a) Weighted sum operation in an eNVM-based synaptic crossbar array structure. (b) Equivalent RC model of a synaptic device.[1]

Project Goals

- Demonstrate a robust neural network can be physically implemented
- Enhance hardware implementation by identifying objects in major data sets showing that the software can be emulated on hardware
- Provide a pipeline leading into future developments of hardware implemented neural networks

Methods and Procedures

Hardware	Software
◗ Design 32X32 subarray from Software results with Eagle schematic and layout ◗ Solder multiplexers and surface mount resistors to board ◗ Use micro-controller to work with subarray	◗ Pretrain a deep neural network on CIFAR10 object recognition dataset ◗ Record weights of the nodes at the subarray ◗ Create interface for the microcontroller to work with the PCB and computer

Results

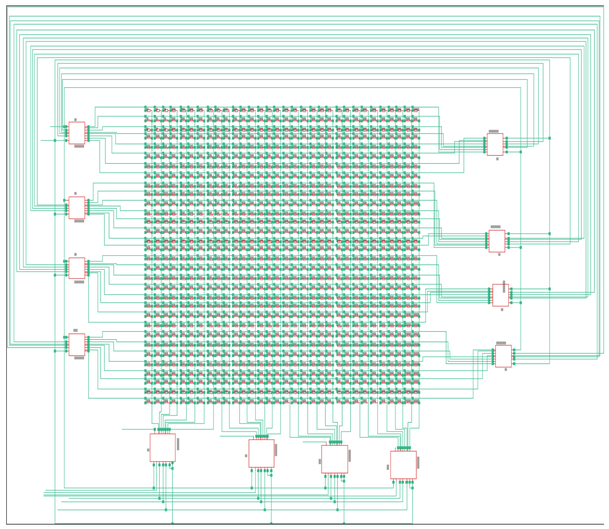

Figure 2: Schematic used to design printed circuit board (PCB) for convolutional neural network. This represents a layer of the network, which each layer performing a separate computation in object or image classification

```
training phase
Train Epoch: 201 [20000/50000] Loss: 0.400587 Acc: 1.0000 lr: 1.00e+00
Train Epoch: 201 [40000/50000] Loss: 0.446838 Acc: 1.0000 lr: 1.00e+00
Elapsed 742224.32s, 3674.38 s/epoch, 14.70 s/batch, ets 202090.78s
testing phase
        Epoch 201 Test set: Average loss: 11.4786, Accuracy: 9231/10000 (92%)
training phase
Train Epoch: 202 [20000/50000] Loss: 0.270396 Acc: 1.0000 lr: 1.00e+00
Train Epoch: 202 [40000/50000] Loss: 0.534952 Acc: 1.0000 lr: 1.00e+00
Elapsed 745909.43s, 3674.43 s/epoch, 14.70 s/batch, ets 198419.26s
testing phase
        Epoch 202 Test set: Average loss: 11.3925, Accuracy: 9239/10000 (92%)
training phase
Total Elapse: 746636.91, Best Result: 92.000%
```

Figure 3: Results of model training on CIFAR10

Future Work

- Create an interface that will allow us to display results on a computer
- Print out the PCB wire to ADC on the physical board
- Finish microcontroller interface and wire to PCB
- Test the neural network on other datasets to determine how well it compares with software
- Analyze results to see if it there is a minimum decrease in accuracy compared to software implementation

Acknowledgment

[1] P. Chen, X. Peng and S. Yu, "NeuroSim: A Circuit-Level Macro Model for Benchmarking Neuro-Inspired Architectures in Online Learning," in *IEEE Transactions on Computer-Aided Design of Integrated Circuits and Systems*, vol. 37, no. 12, pp. 3067-3080, Dec. 2018.

Georgia Tech School of Electrical and Computer Engineering
College of Engineering

19

Improving the Performance of Online Predictive Modeling of the Thermal Effect of Bio-implants

Michael Goldstein, Solomon Martin, Nikhil Patel, Alex Xu

Faculty Advisor: Dr. Ying Zhang, Phd Advisor: Ayça Ermiş

Sensors and Intelligent Systems Lab

Opportunity Research Scholars' Program

School of Electrical and Computer Engineering

Georgia Institute of Technology

Objective

- Reduce instability of identification algorithm:

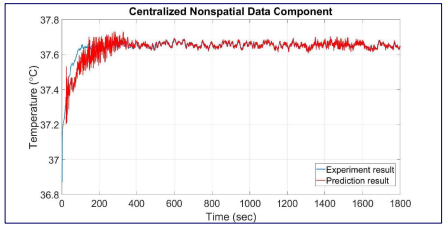

Figure 1. Unstable non-spatial temperature prediction using RLS

- Proposed improvement areas:
  - Alternative RLS filters
  - Sensor weights matrix
  - Kernel models for KRLS filters
  - COMSOL model

Background

- Increasingly complex medical implants will dissipate more heat
- A 0.8° C difference between device and tissue can lead to damage
- Application includes medical implants for monitoring and stimulus purposes.

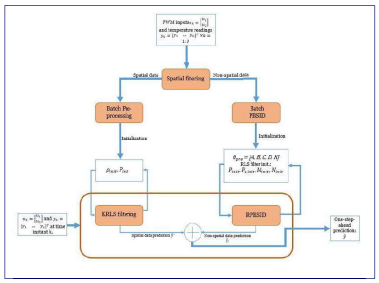

Figure 2. Current prediction algorithm that splits data into spatial and non-spatial components.

Methodology

- Fast Transversal Recursive Least Squares -> Fast Array
  - Initial solution to improve convergence
  - Inherent positive feedback mechanism causes instability
  - Fast Array solution derived from Laguerre model - better numerical conditioning
- Kernel Function
  - Remap to higher dimension for better linearity
  - Adaptive parameters for kernel functions
  - VecNorm: Remap input as norm to saved vector in dictionary.
  - Gaussian VecNorm: gaussian distributed VecNorm.
- Weight Matrix
  - Estimate temperature by relating sensors in space
  - Implement Gaussian Distribution
- Pre-processing
  - Format data for quicker/more accurate predictions
    - 1) Normalization 2) Detrending 3) Regularization
- COMSOL
  - Add characteristics to model for more accurate simulation
  - Homeostatic cooling via blood flow

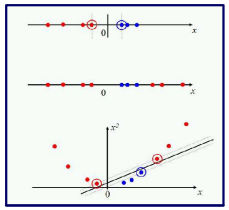

Figure 3. Showcase of kernel function.

Results

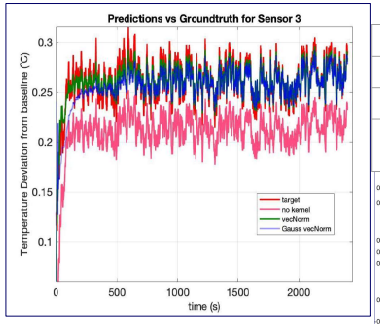

Figure 4. Spatial data prediction performance of Sensor 3 using kernel function as example performance showcase.

Table 1. MSE For Sensor 3 Prediction

Algorithm	MSE (℃)
No Kernel	2.66758e-3
VecNorm	4.5916e-5
Gaussian VecNorm	1.3904e-4

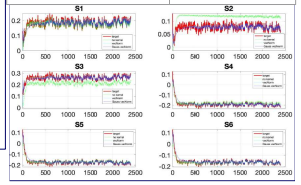

Figure 5. Spatial data prediction performance of all sensors.

Figure 6. Basic COMSOL model with flow cooling added, after simulation

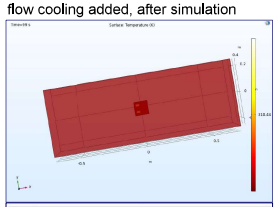

Material	Selection
Copper (mat1)	No domains
FR4 (Circuit Board) (...	Domains 4–5
Water, liquid (mat3)	Domain 2
Air (mat5)	Domain 1
SiO2 - Silicon oxide (...	Boundaries 5–9, 42
SiO2 - Silicon oxide 1...	Domains 6–7
Copper 1 (mat8)	No domains
Si - Silicon (mat9)	Domain 3

Table 2. Materials used in model above

Conclusions & Future

- Implemented Kernel RLS algorithm
  - More accurate prediction result can be achieved with properly designed and tuned kernel.
  - Future: Selection of Kernel Function and auto update of kernel function parameters.
- Added cooling via flow to basic COMSOL model
  - Future: Extend improvements to a more brain analogous model

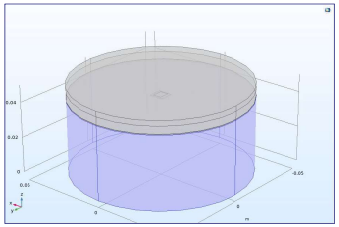

Figure 7. COMSOL model to improve, composed of scalp, skull, and brain materials

- Spatial heat sensor weights must be scaled to properly account for them
- Fast array RLS is more suited to improve convergence
  - Future: Successfully implement FARLS to improve convergence

Acknowledgement

This project has been partially funded by NSF under Grant ECCS-1711447 and Grant CNS-1253390.

References

[1] R. Saracco, "An Antenna for the Brain," IEEE Future Directions, October, 2017. Accessed on: Oct. 28, 2019. [Online]. Available: https://cmte.ieee.org/futuredirections/2017/10/21/an-antenna-for-the-brain/

[2] A. Ermis, Y. Lai, X. Pan, R. Chai and Y. Zhang, "Recursive Subspace Identification for Online Thermal Management of Implantable Devices," *57th Annual Allerton Conference on Communication, Control and Computing*, Monticello, IL, USA, Sept. 24-27, 2019.

[3] "Kernel Statistics," Wikipedia. Accessed on: Oct. 28,2019. [Online]. Available: https://en.wikipedia.org/wiki/Kernel_(statistics)